

Experimental investigation of on-site degradation of crystalline silicon PV modules under Malaysian climatic condition

M A Islam^{a,b}, M Hasanuzzaman^{a*} & Nasrudin Abd Rahim^{a,c}

^aUM Power Energy Dedicated Advanced Center, Level 4, Wisma R & D, University of Malaya, Kuala Lumpur 59990, Malaysia

^bInstitute of Graduate Studies, University of Malaya, Kuala Lumpur 50603, Malaysia

^cRenewable Energy Research Group, King Abdulaziz University, Jeddah, Saudi Arabia

Received 24 May 2017; accepted 3 November 2017

Photovoltaic (PV) power plant capacity is growing very fast in Malaysia. The operating capacity of a PV plant digresses from the installed capacity after several years of operation. The degradation rate of different poly and mono crystalline silicon PV modules due to real field aging at various time spans has been detected by EL imaging, maximum power measurement and dark *I-V* analysis. The obtained degradation values of PV modules are 1.78, 7.06, 13.92, 17.04 and 17.42% due to ageing at a period of 8 months, 16 months, 4 years, 9 years and 11 years, respectively. The reason behind this degradation is attributed to the reduction of shunt resistance which declines gradually as result of aging. The degradation rate of a PV module has been estimated as 18.61% after 21 years of aging. Temperature coefficient of maximum power of PV module also degrades due to aging. And the rate of temperature coefficient of maximum power degradation decreases with the increase of aging period.

Keywords: PV module degradation, Aging, EL image, Dark *I-V*, Shunt resistance, Temperature coefficient

1 Introduction

Photovoltaic (PV) module lifetime, together with the system price, the annual solar irradiance, and the capital interest rate, is one of the vital factors in determining the cost of solar electricity. That is why; lifetime forecast related issues remain a concern of interest to many researchers¹. The major two factors that determine the cost-effective energy harvesting from the solar radiation are (i) efficiency at which sunlight is converted into power and (ii) how this conversion relationship changes over time due to aging. Normally PV solar modules are degraded due to field aging through several ways, such as discoloration of encapsulant in several degrees ranging from yellow to dark brown, degradation of the anti-reflective (AR) coating, formation of hotspots², moisture intrusion, delamination of encapsulant and corrosion³, tears and bubbles in the back sheet and cracks in PV cell caused by mechanical stress, etc. While several causes of degradation effects may co-exist in the same module, even in the same cell⁴, optical/physical, electrical and thermal degradation effects may be linked with power and performance degradation of the PV module⁵. Generally, the estimated lifetime of the PV modules is

about 20–25 years. PV modules power should not drop more than 20% of their nominal power over this period^{6,7}. Different degradation rates due to aging have been found in different locations⁸. Sánchez-Friera *et al.*⁹ reported an average degradation rate of PV module maximum power 0.96% per year due to aging in Malaga, Spain. In Manfredonia, Italy, maximum 2.16% degradation rate per year has been detected⁵. Degradation rate on account of aging of PV module is not linear and the rate is decreased exponentially with the aging year¹⁰.

On the other hand, PV cell performance decreases with the increase of cell temperature. Band gap of PV cell material reduces with increase of temperature and the open circuit voltage, output power and efficiency of cell degraded¹¹. The temperature coefficient of PV cell parameters is varied according to the type of solar cells¹². There are several researches which have been carried out to evaluate the temperature dependent performance of the solar cell. Kalogirou and Tripanagnostopoulos¹³ reports that for mono crystalline and poly crystalline silicon solar cells, the efficiency decreases by about 0.45%/°C and for amorphous silicon cells about 0.25%/°C increase of cell temperature. Therefore, both aging and temperature effects are two critical factors for the financial analysis of the PV power plant.

*Corresponding author (E-mail: hasan@um.edu.my)

Erroneousness in determined degradation rates leads directly to increased financial risk¹⁴. In addition, the temperature coefficient of PV solar module also degrades due to long time filed ageing¹². Malaysia is very potential region for the PV based energy harvesting process and has become the world's third-largest producer of PV modules and components¹⁵. Nonetheless the degradation feature of PV module due to onsite aging in Malaysian climate condition is rare in literature. The objective of this research is to investigate the detail onsite aging feature of PV module by evaluating (i) internal conditions of each cell within the module and (ii) power and efficiency and temperature coefficient degradation.

2 Experimental Procedure

2.1 Meteorological conditions of PV plant site and PV module specification

The real features of aging degradation of PV modules have been investigated by using different PV modules from a 4-kW PV power plant installed at the Solar Garden, University of Malaya Power Energy

Dedicated Advanced Center (UMPEDAC), Kuala Lumpur, Malaysia. The geographical location of the plant is in between 101.667° east longitude and 3.117° north latitude. All modules were set up at 15° inclined to the horizontal. Both mono- and polycrystalline PV modules, field aged for different span of time, have been used to carry out the investigation. Detail module specifications at standard testing conditions are showed in Table 1. Table 2 shows the climate conditions data of the PV plant site. Average maximum temperature is 26 °C in May while minimum is 24.9 °C in December. Annual average solar insolation is 4.90 kWh/m²/day on the horizontal surface and annual average wind speed and relative humidity are 2.63 m/s and 81%, respectively.

2.2 Theory of electroluminescence imaging

Electroluminescence imaging is a versatile technique for spatially resolved analysis of different electrical properties of PV module and individual cell within the module. Photovoltaic module performances such as shunt resistance and series resistance¹⁷, micro

Table 1 — Specification of PV modules taken as sample in the experiment.

Module specifications	Module A	Module B	Module C	Module D
Manufacturer	ENDAUPV	SHAIYANG	MITSUBISHI	SHELL SOLAR
Material	Polycrystalline Silicon	Monocrystalline Silicon	Polycrystalline Silicon	Monocrystalline Silicon
Number of Cell	6×10	4×9	4×9	4×9
Module Size (mm)	1666×997×42	1200×545×35	1495×674×46	1200×527×46
Maximum Power	250W	90W	125W	85 W
V_{oc} (V)	36.96	22.03	21.8	22.2
I_{sc} (A)	8.8	5.30	7.9	5.45
V_{mp} (V)	31.26	18.36	17.3	17.2
I_{mp} (A)	8.0	4.90	7.23	4.95
Size of cell (mm)	156×156	125×125	156×156	125×125
Temperature coefficient	0.45	0.549	0.452	0.43

Table 2 — Monthly 22 years average climate condition of the PV plant site¹⁶.

Month	Averaged Insolation (kWh/m ² /day)	Temperature (°C)			Average wind speed (m/s)	Average RH (%)
		Average	Average Maximum	Average Minimum		
January	4.79	25.00	28.00	22.10	3.64	77.40
February	5.37	25.70	28.90	22.50	3.08	73.90
March	5.42	25.90	28.90	22.90	2.68	77.50
April	5.27	25.90	28.70	23.30	1.83	82.20
May	5.11	26.00	28.70	23.40	1.80	83.00
June	4.98	25.60	28.40	22.90	2.58	82.70
July	4.92	25.20	28.00	22.70	2.63	83.10
August	4.87	25.30	28.20	22.80	2.81	83.00
September	4.88	25.40	28.20	22.80	2.25	82.50
October	4.76	25.60	28.30	23.10	2.00	82.10
November	4.36	25.40	27.90	23.10	2.67	83.10
December	4.17	24.90	27.50	22.50	3.66	81.70
Annual	4.90	25.50	28.30	22.80	2.63	81.00

crack¹⁸, even diffusion length of minority carrier of PN junction^{19,20} have been explored through EL imaging. Individual PV cell performance within the module depends on the PN junction performance which depends on diffusion length of minority carrier²⁰. A one to one relationship between EL intensity and minority carrier diffusion length has been reported, which yields a quantitative analytical method for the detection of degradation of PV cells¹⁹. Mochizuki *et al.*²¹ proposed a quantitative open-circuit voltage mapping method from EL intensity of PV module. The authors have used a reference module to calibrate relation between module parameter and EL intensity. When the *p*-type PV cell is forward biased at voltage greater than the built-in potential of *p-n* junction, then minority carriers of *p*-type base cross the junction and enter to *n*-type. The minority charge carrier electrons recombine with holes by releasing photon light. So, the EL intensity for a pixel is proportional the number of radiative recombination of electron hole pairs which depends on the number of transferred minority carriers *N* due to forward bias. The total number minority charge carrier at a pixel along the depth at a distance *x* from the *p*-side edge can be expressed as follows:

$$n(x) = n_p(0) \exp(-x/L_e) \quad \dots (1)$$

where $n_p(0)$ is the number of (electron) injected from *p* side edge of the *p-n* junction. L_e localized effective diffusion length which involves the effect of defects, impurities, and the surface recombination velocity at the rear surface, etc. The total number of minority charge carrier for the pixel '*N*' is as:

$$N = \int_0^W n_p(0) \exp(-x/L_e) dx \quad \dots (2)$$

$$N = n_p(0) L_e [1 - \exp(-W/L_e)] \quad \dots (3)$$

where *W* is the thickness of the cell. The term $[\exp(-W/L_e)]$ is considered to be much less than 1. Then:

$$N = n_p(0) L_e \quad \dots (4)$$

$n_p(0)$ at an applied forward voltage *V* has been expressed as²²:

$$n_p(0) = n_p \exp(eV/kT) \quad \dots (5)$$

where n_p is equilibrium minority charge carrier in *p* layer, *e* is electron charge, *k* is Boltzmann constant and *T* is temperature.

The EL intensity for a pixel of PV cell is proportional to the equilibrium minority charge carrier and effective diffusion length and PV cell performance also depend on these parameters. So maximum power (P_{max}) of PV cell is proportional to summation of total pixel's EL intensity and mean intensity of pixels of EL image is proportional to the (P_{max}) per unit area of the PV cell because total number of pixel is equivalent to the cell area:

$$E_{mean} \propto \frac{P_{max}}{A_{cell}} \quad \dots (6)$$

$$E_{mean} = C \times \frac{P_{max}}{A_{cell}} \quad \dots (7)$$

where E_{mean} is the mean pixel intensity of the EL image, *C* is a calibration factor, P_{max} is maximum power and A_{cell} is total cell area of the PV module. The value of *C* can be determined from the EL image of a new non-degraded PV module.

2.3 Experimental investigation

2.3.1 EL imaging

An electroluminescence (EL) imaging setup package is used to analyze the individual cell performance of the aged modules. It contains dark room with CCD camera, programmable power supply and computer with measurement software. A Minolta MD W. Rokkor objective with a focal length of 35 mm and a maximum *F* number of *f*/1.8 is equipped with the CCD camera. The camera is mounted on a tripod which can move freely through a tunnel. The camera scans the whole PV module by moving in the longitudinal direction. By a single shot camera can cover a distance of 30 cm and several shots are done for a close-up measurements of the full module scan. Number of shot depends on the module length. The 5.5 m tunnel length allows the measurement of all common panel sizes of up to 2 m×2 m. Programmable DC power supply with a maximum voltage output of 150 V and a maximum current output of 15 A has been used for the PV module forward biasing. The integrated synchronization module allows the control of the EL camera as well as the communication with the measurement software. Photovoltaic module is placed inside the dark room and connected with cable of DC power source for forward biasing. Doors of the dark room are closed during the imaging process. For every shot, PV module is biased with 50 V and camera captures the EL intensity. The EL intensity of individual cell has been measured by means of selecting the whole cell by marquee tool as shown in

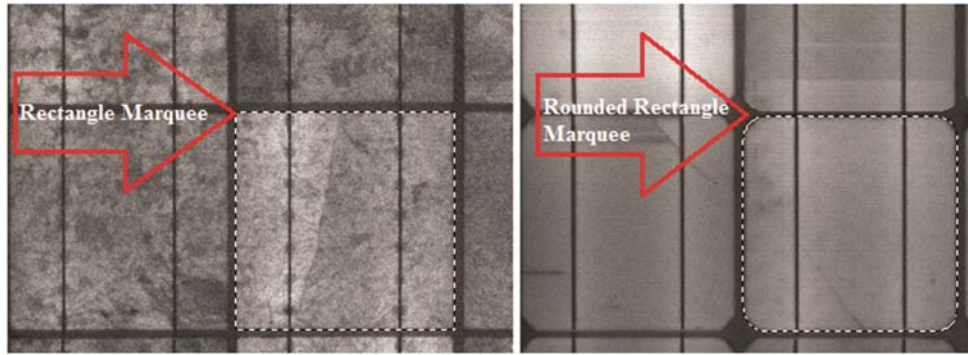


Fig. 1 — EL intensity measurement of individual cells with a polycrystalline (left) and monocrystalline (right) PV module.

Fig. 1. For polycrystalline PV module, the rectangle marquee tool and for mono crystalline PV, the rounded rectangle has been used. The mean intensity of individual cell has been detected from the histogram of respective cell image²³.

2.3.2 Maximum power (P_{max}) measurement

Output performances different degraded PV modules were tested during the sunny days at real operating condition by using maximum power point tracker (MPPT). Simultaneously, the solar radiation, module back and front surface temperature and ambient temperature were also monitored by pyranometer and thermocouples through a data logger. The specification of MPPT is shown in Table 3. K-type thermocouples (welded-tips and PTFE coated) are used to measure the top and bottom surface temperature of the solar module. The measuring capacity range of the thermocouple is $-75\text{ }^{\circ}\text{C}$ to $250\text{ }^{\circ}\text{C}$ ($-40\text{ }^{\circ}\text{F}$ to $167\text{ }^{\circ}\text{F}$). The pyranometer (LI-COR PY82186) is used to measure the solar radiation. The irradiance measurement capacity of the pyranometer is 0 to 1280 W/m^2 within an operating temperature range of $40\text{ }^{\circ}\text{C}$ to $75\text{ }^{\circ}\text{C}$. Maximum power of PV module was measured in real operation condition and the measured values were converted to STC according to IEC 61215 based on the temperature coefficient. The temperature coefficient was detected from the P_{max} at 1000 W/m^2 versus PV cell temperature curve.

2.3.3 Dark I-V measurement

Dark I-V (DIV) characteristic has been measured at room temperature $25\text{ }^{\circ}\text{C}$. During the DIV testing, the PV module surface was covered with a hard board paper. The DC power supply was adjustable and both current and voltage can be regulated to get desired output. The output voltage and current range of the

Table 3 — Specification of maximum power point tracker.

Parameter	Minimum value	Maximum value
Open circuit voltage (V_{oc})	1 V	600 V
Short circuit current (I_{sc})	0.5 A	7 A
Maximum power (P_{max})	0 W	3000 W

power supply are 0-30 V and 0-3 A, respectively. Biasing current was calculated from the voltage generated due to a resistor in series connection.

2.4 Mathematical formulation

2.4.1 PV module degradation

Degradation D of PV module has been calculated as:

$$D = (E_{mean0} - E_{mean}) / E_{mean0} \times 100\% \quad \dots (8)$$

$$E_{mean0} = \frac{P_{max}(STC)}{A_{cell}} \times C \quad \dots (9)$$

where E_{mean0} is mean EL intensity at non-degradation condition which is obtained from the nominal value of P_{max} at STC and total cell area A_{cell} of the PV module. E_{mean} is mean EL intensity of degraded PV module and C is correlation factor adjusted by new PV module EL image.

2.4.2 Solar cell temperature and temperature coefficient of P_{max}

Energy absorbed by the upper layer of the PV module can be calculated by the formula as proposed by Dubey and Tay²⁴ and Teo *et al.*²⁵:

$$E_{ab} = \tau_g \alpha_{sc} p_{sc} G A_{cell} \quad \dots (10)$$

The energy transferred from the top surface of the PV module as a result of the convection process is:

$$E_{ctop} = U_{sca} (T_{sc} - T_a) A_{cell} \quad \dots (11)$$

The total energy conducted from the top surface to the back of the PV module is:

$$E_b = U_t (T_{sc} - T_b) A_{cell} \quad \dots (12)$$

The electrical energy converted from the incident solar radiation is:

$$E_c = \eta_{sc} p_{sc} G A_{cell} \quad \dots (13)$$

Thus, the energy balance equation for the top surface of the module can be written as:

$$E_{ab} = E_{ctop} + E_b + E_c \quad \dots (14)$$

The formula for the solar cell temperature can be derived from Eqs (10)–(14) as follows²⁶:

$$T_{sc} = \frac{p_{sc} G (\tau_g \alpha_{sc} - \eta_{sc}) + (U_{sca} T_a + U_t T_b)}{(U_{sca} + U_t)} \quad \dots (15)$$

Solar cell temperature determining parameters and respective values are shown in Table 4. The temperature coefficient of maximum power (γ) has been calculated by using following equation:

$$\gamma = \left[\frac{P_{max}(STC) - P_{max}(T_{sc}, 1000W/m^2)}{T_{sc} - 25^\circ C} \right] \div P_{max}(STC) \times 100\% \quad \dots (16)$$

Degradation rate of temperature coefficient of P_{max} (DR_γ) is calculated by Eq. (17) where Y_{age} is the aging period in year:

$$DR_\gamma = \frac{\gamma - \gamma(STC)}{\gamma(STC)} \div Y_{age} \times 100\% \quad \dots (17)$$

Table 4 — Solar cell temperature determining parameters and their respective value^{24,26}.

Parameters	Values
Transmissivity of glass (τ_g)	0.96
Solar module absorptivity (α_{sc})	0.9
Overall heat transfer coefficient through glass cover from top surface of module to ambient (U_{sca})	7.14 W/m ² K
Overall heat transfer coefficient from top surface of module to tedlar back surface (U_t)	150 W/m ² K

3 Results and Discussion

3.1 EL image

Figure 2 shows the EL image of a type “A” EPV-250 brand new PV module. The mean EL intensity of individual cell is presented in the right side. Different values of mean EL intensities are obtained for different cells and the values are in the range from 140 to 200. This is due to dissimilar doping concentration of different cells. Average of all cells’ mean EL intensity is 170.36 with a standard deviation of 33.43 as presented in Table 5. The nominal “ P_{max} /total cell area” of the PV module is 171.21, from which the calibration factor C in the Eq. (7) has been calculated as 0.99. With this C value and “ $P_{max}(STC)/A_{cell}$ ” value, the mean EL intensity of a brand new non degraded different PV modules has been calculated by using Eq. (9). The mean EL intensity (EL_{mean0}) of A type PV module at non degraded brand new condition has been calculated by using Eq. (9) and the value is count as 169.50 as shown in Table 6. Figure 3 shows the EL image (left) and individual cell performance deviation (%) from the EL_{mean0} value (right) of 8 month field aged PV module type A. There is no crack observed in the PV module. Non-homogeneous individual cell performance has been obtained from the EL image. The negative and positive sign of cell performance indicate the less and more performance compared to the EL_{mean0} . Overall

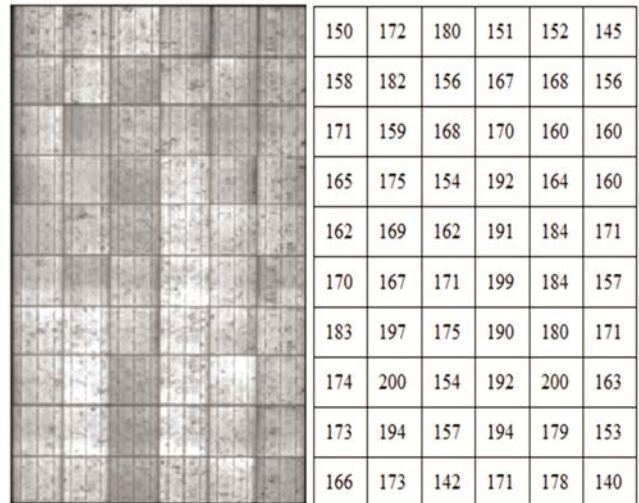


Fig. 2 — EL image and individual cell mean EL intensity of the new unused and “A” type PV.

Table 5 — EL image properties of the new PV modules EPV 250 W.

PV module	Nominal P_{max} at STC (W)	Nominal P_{max} /Total Cell area (W/m ²)	EL image mean intensity count	Calibration factor	Standard deviation
EPV-250	250	171.21	170.36	0.99	33.43

degradation the PV module has been calculated from the average performance of all cells within the module. The degradation value is 1.78% due to 8 month aging. Figure 4 shows the EL image (left) and individual cell performance deviation (%) from the EL_{mean0} value (right) of 16 month aged PV module of type A. Both dark and bright cells are shown. A very

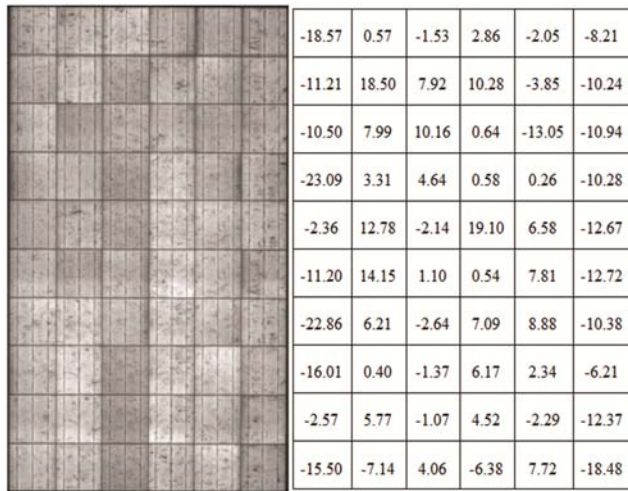


Fig. 3 — EL image and individual cell performance (%) of the 8 month aged “A” type PV module.

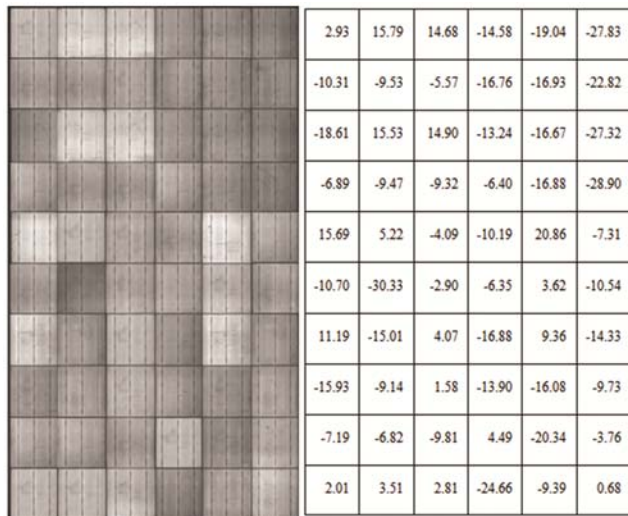


Fig. 4 — EL image and individual cell performance (%) of the 16 months aged “A” type PV module.

small amount of contact finger interruptions are observed throughout PV module²⁷. Highest negative and positive deviations of cell performance from the EL_{mean0} value are -30.33% and 20.86%, respectively. Overall degradation the PV module has been calculated from the average performance of all cells within the module. The average mean EL intensity of total module has been found as 157.53 counts as presented in Table 6. The degradation value is 7.06% due to 16 month aging. Figure 5 shows the EL image (left) and individual cell performance deviation (%) from the EL_{mean0} value (right) of 4 years aged PV module B type. The existence of contact grid problems, namely broken fingers has been revealed more clearly compare to 16 month aged PV module. Dark lines indicate the presence of cracks. Also, the dark regions visible in some solar cells are indicative of the existence of a high recombination region (either due to bulk or surface defects)²⁸. Highest negative and

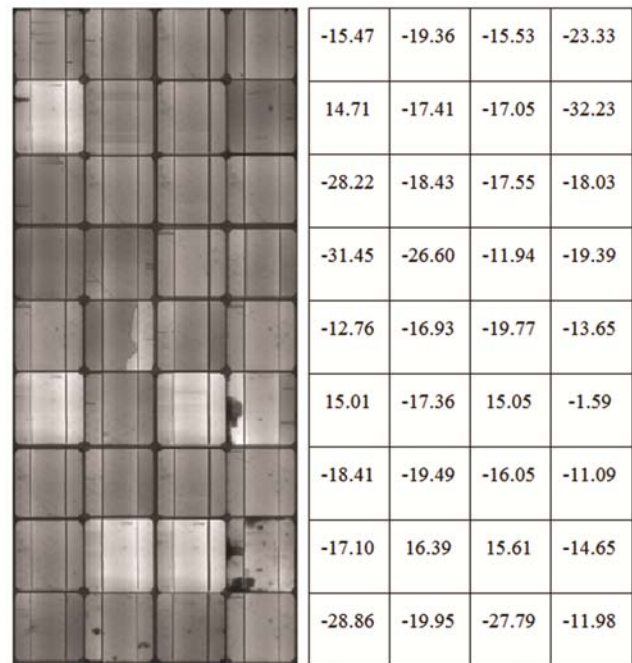


Fig. 5 — EL image and individual cell performance (%) of the 4 years aged B type PV module.

Table 6 — Assessing degradation of PV module from electroluminescence image.

PV module type	Aging period	Mean EL intensity of degraded module	$P_{max}(STC)/A_{cell}$	Mean EL intensity of brand new PV module (from Eq. (9))	Degradation (%) (from Eq. (8))
A	8 month	166.47	171.21	169.50	1.78
A	16 month	157.53	171.21	169.50	7.06
B	4 year	136.35	160	158.4	13.92
C	9 year	117.18	142.68	141.25	17.04
D	11 year	123.53	151.11	149.60	17.42

positive deviations of cell performance from the EL_{mean0} value are -32.23% and 16.39%, respectively. Overall degradation the PV module has been calculated from the average performance of all cells within the module. The average mean EL intensity of total module has been found as 136.35 counts as presented in Table 6. The degradation value is 13.92% due to 4 years aging.

Figure 6 shows the EL image (left) and individual cell performance deviation (%) from the EL_{mean0} value (right) of 9 years aged PV module C type. The highest negative and positive deviations of cell performance from the EL_{mean0} value are -46.87% and 12.88%, respectively. The average mean EL intensity of total module has been found as 117.18 counts as presented in Table 6. The degradation value is 17.04% due to 9 years aging and the degradation rate is 1.89%/year which very closes as reported rate⁵ of 1.87%/year at Italy after 10 years aging. Figure 7 shows the EL image (left) and individual cell performance deviation (%) from the EL_{mean0} value (right) of 11 year aged PV module type “D”. Maximum negative and positive deviations of cell performance from the EL_{mean0} value are -48.18% and 14.99%, respectively. The average mean EL intensity of total module has been found as 123.53 counts and 17.42% degradation is occurred due to 11 years aging. The EL images of polycrystalline type PV module contain some dark and bright spots. On the other hand the EL images of mono crystalline PV show smooth better

homogeneous brightness compared to polycrystalline PV module. This is due to presence of grain boundary related dislocation defect in polycrystalline PV module²⁸. Degradation measurement parameters and their respective values for different aged PV modules are shown in Table 6. Mean EI image intensity has been calculated from the EL image histogram. $P_{max}(STC)/A_{cell}$ obtained from the manufacturer data sheet. Mean EL intensity of brand new PV module has been assessed by Eq. (9). Finally the degradation of respective PV module has been calculated by Eq. (8).

Figure 8 shows the PV module degradation behaviour as a result of varying aging period. The amount of degradation are 1.78, 7.06, 13.92, 17.04 and 7.42% for 8 months, 16 months, 4 years, 9 years and 11 years field aging, respectively. At the initial stage of aging the degradation rate is very high and the rate decreases gradually at higher aging period. Similar behaviour is also reported in literature¹⁰. From the experimental data, a curve has been fitted to estimate the possible degradation at high aging period in Malaysian climatic condition. The estimated degradation after 21 years is 18.61%, which fulfills the manufacturer warranty (< 20%). The degradation rate after at 21 years is 0.86%/year. The rate is comparable with other reports such as 0.96%/year at Patras, Greece after 22 years⁴ and 0.81%/year in

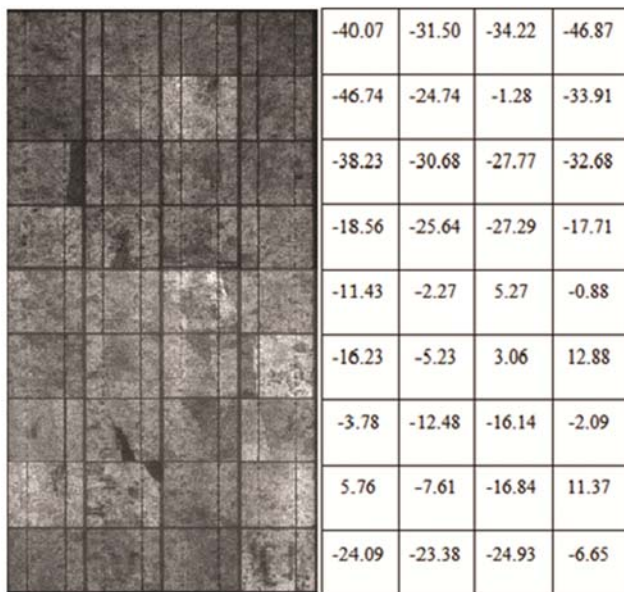


Fig. 6 — EL image and individual cell performance (%) of the 9 years aged C type PV module.

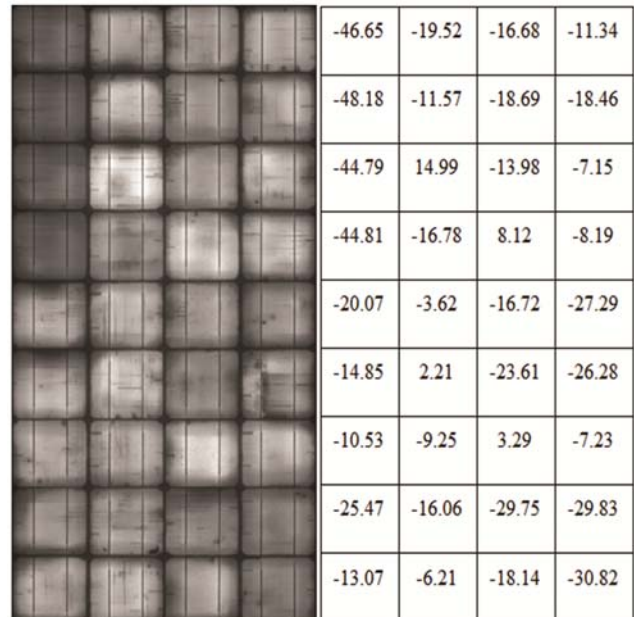


Fig. 7 — EL image and individual cell performance (%) of the 11 years aged D type PV module.

Trinidad, California after 20 years of natural aging²⁹. Table 7 summaries degradation rate of PV modules in different location, which were published previously, together with the results of this work.

3.2 Impact of degradation on the PV plant output

The impact of degradation on the PV plant cash flow has been estimated based on the fixed investment cost of building integrated 12 kWp PV system. The grid connected PV plant system cost includes different sorts such as PV module cost, inverter cost, wiring and racking cost and installation labor cost, etc. Sustainable Energy Development Authority (SEDA) of Malaysia has reported the PV

module and system prices of RM 3.07 and RM 7.79, respectively, in 2015 as shown in Table 8. Annual maintenance cost of PV system has been taken 1% of the total investment cost³¹. Two times inverter replacement has been considered within the 21 years³³. Electricity production from the 12 kWp PV plant has been estimated based on the solar radiation data and PV module type ‘A’ performance shown in Table 1. Different types of losses are occurred for PV system such as inverter loss, DC and AC cable loss, shading and weak irradiance loss, and loss due to dust related deposition.

A total 15% system loss is considered for the PV plant³⁵. Average cash inflow from the PV plant is determined based on electricity sell according to Feed in tariff (FiT) rate effective from 1st January 2017. Rate is RM 0.7243 /kWh and additional bonus RM 0.1395 /kWh due to installation in building. Activation year of this FiT rate is 21 years from the commencement date³⁶. Figure 9 shows a simple cash

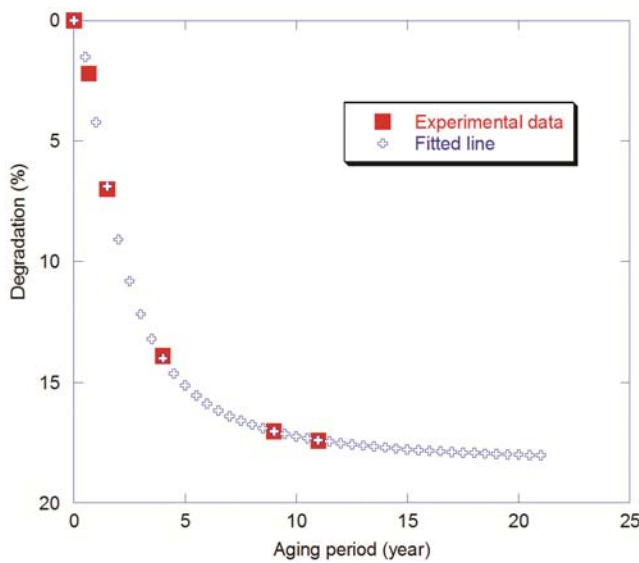


Fig. 8 — Effect of aging period on the degradation of PV module.

Table 8 — Installation cost of ≤ 12kW PV plant in Malaysia³⁴

Cost category	Average (RM/W)	Low (RM/W)	High (RM/W)
Module	3.07	2,13	4,80
Inverter	1	0,46	1,48
Racking, wiring, etc.	0.94	0,34	1,81
Installation	1.36	0,57	2,73
Customer acquisition	0.02	0,16	0,25
Permitting, contracting, financing, etc.	0.11	0,02	0,39
Profit	1.29	0,12	3,06
Total	7.79		

Table 7 — Degradation rates of PV modules in different locations.

Reference	Type PV module	Aging period	Degradation Rate (%/year)	Location
Ndiaye <i>et al.</i> ³⁰ (2014)	Monocrystalline	1.3	0.22	Dakar, Senegal
	Polycrystalline	3.4	1.62	
	Monocrystalline	4	2.99	
	Polycrystalline	4	2.96	
Bandou <i>et al.</i> ⁷ (2015)	Mono C-Si	28 years	1.22	Algeria
Limmanee <i>et al.</i> ³¹ (2017)	Multi c-Si	4	1.2	Thailand
	HIT	4	1.3	
	Microphorm	4	1.8-6.1	
	CIGS	4	1.7	
Charrouf <i>et al.</i> ³² (2017)	Monocrystalline silicone	5 years	3.63	Algeria
	Monocrystalline silicone	10 years	1.74	
Present study (2017)	Poly crystalline	8 months	2.64	Kuala lumpur, Malaysia
	Poly crystalline	16 months	5.30	
	Monocrystalline	4 years	3.48	
	Polycrystalline	9 years	1.89	
	Monocrystalline	11 years	1.58	

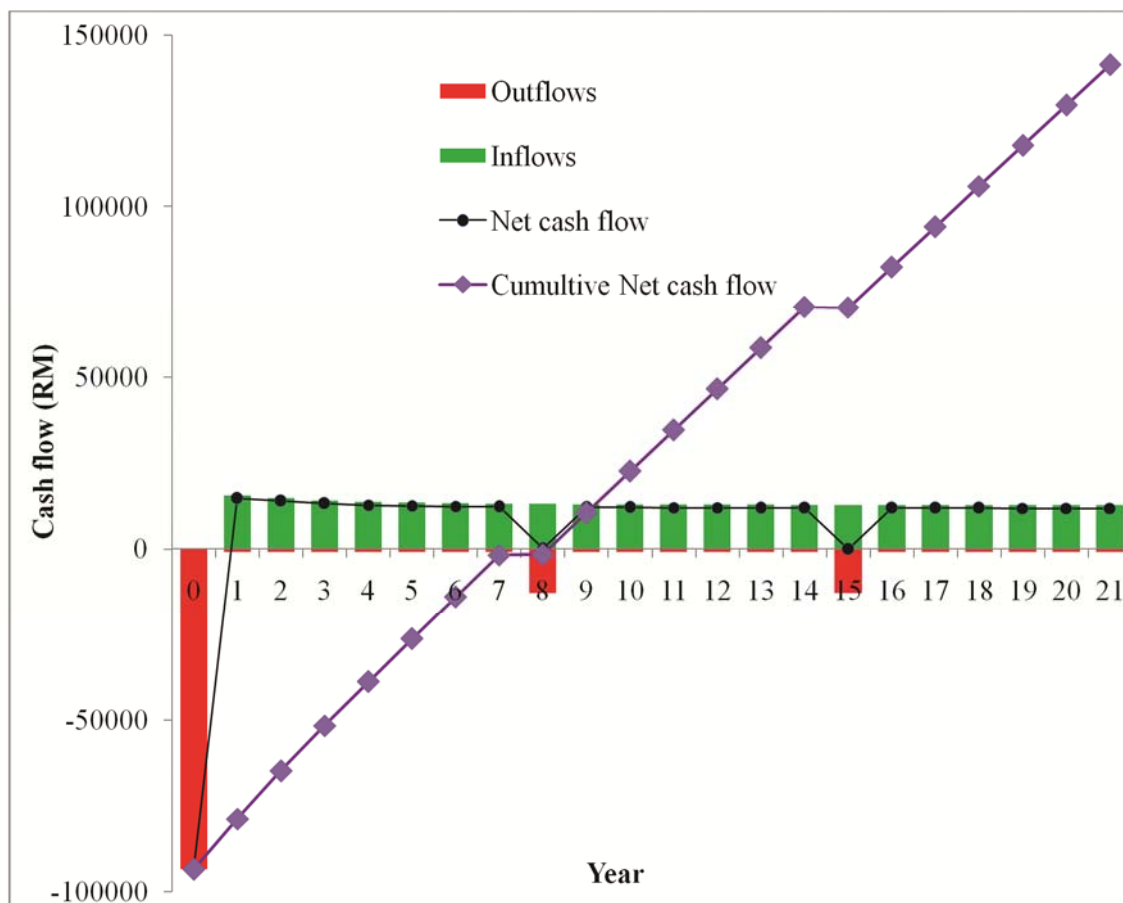


Fig. 9 — Simple cash flow of 12 kW BIPV power plant.

flow for the 12 kW BIPV system. Outflow and inflow are responsible for cost and money return of the system, respectively. Initially the outflow is RM 93480 due to installation cost and every year RM 935 as an operating cost. Inflow of PV plant is based on the money return from electricity sell which decreases gradually per year according to the degradation rate of PV module as estimated in Fig. 8. Net cash is a summation of cash inflow and outflow. Inverter replacement cost is added in 8th and 15th years which increase the outflow of the plant. Net cash flow reduced to RM 175 in 8th year and in the 15th year the value become negative as -RM 103. Up to 8th year, the cumulative net cash is negative and at 9th year the value crosses the baseline which is the payback period of the plant. The overall profit of the plant states at 9th year and total cumulative profit of the plant is RM 1, 41,392 after 21.

3.3 Shunt resistance

The shunt resistance of different aged PV module has been calculated by measuring $I-V$ at dark condition.

Semi logarithmic current density (J) versus voltage (V) curves of different aged PV module are revealed in Fig. 10. The shunt resistance has been determined by taking the JV data near zero voltage where the $J-V$ characteristic is a clear straight line. From the linear fit model, the slope (dJ/dV) of the straight line has been calculated and the inverse of the slope is the shunt resistance. The obtained shunt resistance values of different PV modules are 125, 86.95, 60.39, 10.15, 4.04 and 3.36 $k\Omega m^2$ for new, 8 months, 16 months, 4 years, 9 years and 11 years aging, respectively. Shunt resistance gradually decreases with increase of aging periods due to increase of different types of defects as revealed by respective EL images. Decrease of shunt resistance due to aging is also reported for crystalline PV module³⁷. The possible cause of severe power loss due aging is the low value of shunt resistance.

3.4 Maximum power temperature coefficient

Solar cell temperature dependent P_{max} behaviour of different PV modules aged at different periods (such as 16 months, 4 years, 9 years and 11 years) is shown

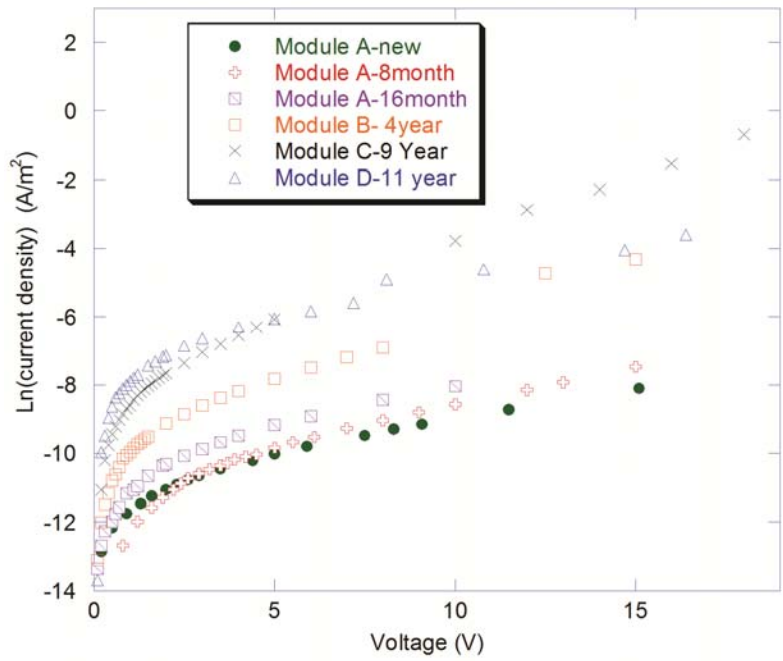


Fig. 10 — Effect of different aging period on the semi logarithmic dark $J-V$ characteristics of PV modules.

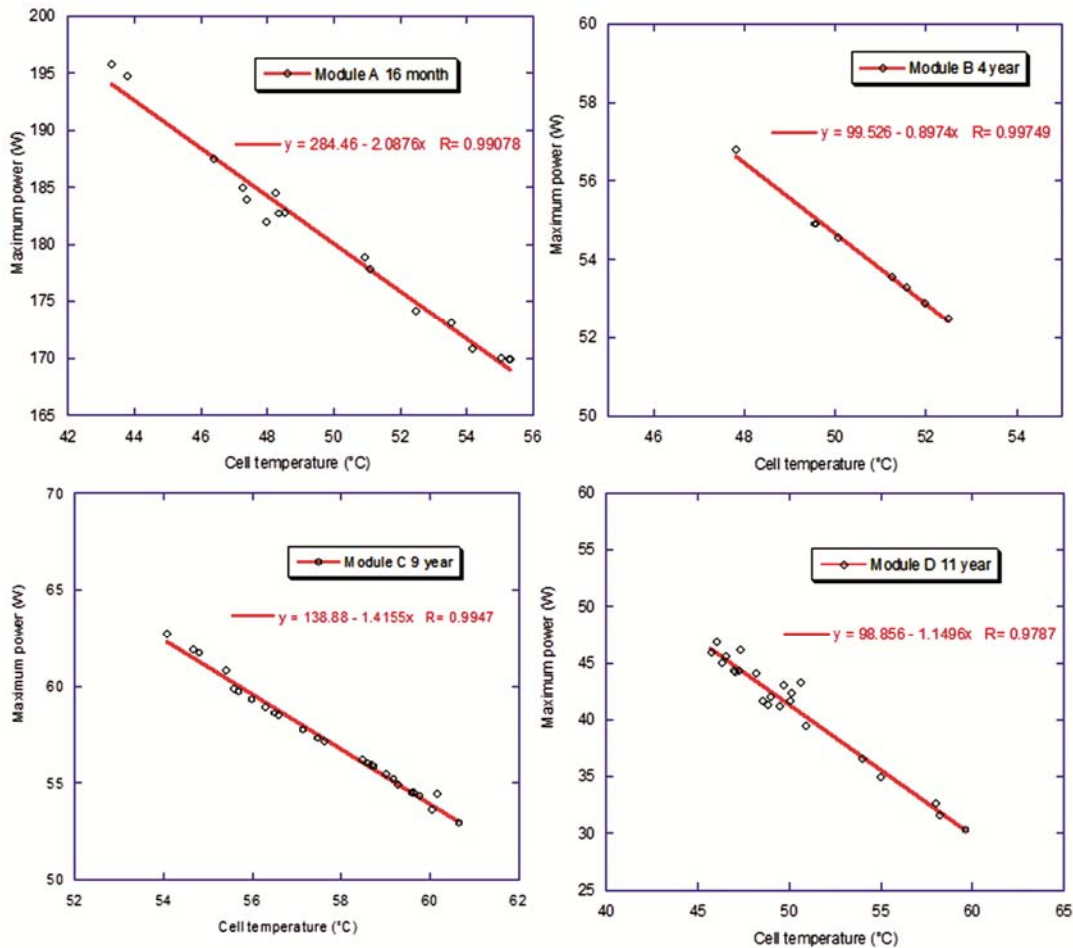


Fig. 11 — Effect of cell temperature on the maximum power output (at $1000 \text{ W}/\text{m}^2$ irradiance) of PV modules aged at different periods. in Fig. 11. From the linear curve fitting and using Eq. (16),

the temperature coefficient of P_{\max} (γ) has been determined. The obtained γ values are 0.898, 1.164, 1.37 and 1.468% for the PV module of 16 months, 4 years, 9 years and 11 years aged, respectively. PV module performance decreases at high temperature because of band gap reduction at high temperature³⁸. The γ value depends on the band gap reduction rate with temperature which depends on the semiconductor materials properties. Due to aging, temperature dependent band gap shrinkage resistant property might be degraded and consequently γ value increases. Initially the increasing rate per year of γ is high and then at higher aging period, the rate decreases gradually. The obtained degradation rate of γ values of PV module under ageing at 16 month, 4 years, 9 years and 11 years are 75%, 28%, 22.56% and 25% per year, respectively.

4 Conclusions

Degradation behaviour of different crystalline PV module aged over different periods in Malaysian climate has been investigated through EL imaging, dark I - V , and cell temperature dependent maximum power measurement processes. The following inferences have been made from the present study:

- (i) The EL images of both polycrystalline and mono crystalline PV module showed that various types of defects in solar cells are possible, such as contact grid problem, grain boundary related dislocations and cracks, etc. The contact grid problems and cracks increase as a result of long time field aging.
- (ii) The obtained degradation values of PV modules are 1.78, 7.06, 13.92, 17.04 and 17.42% due to ageing at a period of 8 months, 16 months, 4 years, 9 years and 11 years, respectively. The reason behind this degradation is the reduction in shunt resistance which declines gradually as result of aging.
- (iii) Degradation versus aging period curve shows characteristic. The estimated degradation from fitted line of a PV module after 21 years is 18.61%.
- (iv) Temperature coefficient of P_{\max} of PV module also degrades due to aging and the rate of degradation of temperature coefficient of P_{\max} also decreases with the increase of aging period.

Abbreviation:

A_{cell}	Area of solar cell (m^2)
DR_{γ}	Degradation rate of temperature coefficient of maximum power

E_{ab}	Total energy (W) absorbed by module top surface
E_{b}	Total energy (W) transferred by conduction and convection from top surface to bottom surface
E_{ctop}	Total energy lost (W) by convection from top surface to ambient
E_{e}	Electrical energy (W) produced by module
E_{mean}	Mean EL intensity
E_{mean0}	Mean EL intensity at non degradation condition
EL	Electroluminescence
G	Incident irradiation (W/m^2)
MPPT	Maximum power point tracker
PID	Potential induced degradation
PV	Photovoltaic
p_{sc}	Packing factor of solar module
STC	Standard test condition
T_{a}	Ambient temperature ($^{\circ}\text{C}$)
T_{b}	Tedlar back surface temperature ($^{\circ}\text{C}$)
T_{sc}	Solar module top surface temperature ($^{\circ}\text{C}$)
U_{sca}	Overall heat transfer coefficient through glass cover from module top surface to ambient ($\text{W}/\text{m}^2\text{K}$)
U_{t}	Overall heat transfer coefficient from module top surface to tedlar back surface ($\text{W}/\text{m}^2\text{K}$)
Y_{age}	Aging period in year
Greek letter	
τ_{g}	Transmissivity of glass
α_{sc}	Absorptivity of solar module
η_{sc}	Electrical efficiency of solar module
α_{t}	Absorptivity of tedlar back sheet.
γ	Temperature coefficient of P_{\max}

References

- 1 Skoczek A, Sample T & Dunlop E D, *Prog Photovolt*, 17 (2009) 227.
- 2 Simon, M & Meyer E L, *Sol Energy Mater Sol Cells*, 94 (2010) 106.
- 3 Quintana M A, King D L, McMahon T J & Osterwald C R, *Commonly observed degradation in field-aged photovoltaic modules*, IEEE 29th Photovoltaic Specialists Conference, New Orleans, Louisiana, 19-24 May 2002.
- 4 Kaplani E, *Int J Photoenergy*, 2012 (2012) 11.
- 5 Parretta A, Bombace M, Graditi G & Schioppo R, *Sol Energy Mater Sol Cells*, 86 (2005) 349.
- 6 Thevenard D & Pelland S, *Sol Energy*, 91 (2013) 432.
- 7 Bandou F, Arab A H & Belkaid M S, *Int J Hydrogen Energy*, 40 (2015) 13839.
- 8 Manganiello P, Balato M & Vitelli M, *IEEE Trans Ind Electron*, 62 (2015) 7276.
- 9 Sánchez-Friera P, Piliouguine M & Peláez J, *Prog Photovolt*, 19 (2011) 658.
- 10 Jordan D C, Silverman T J, Sekulic B & Kurtz S R, *Prog Photovolt*, 25 (2017) 583.
- 11 Radziemiska E, *Renew Energy*, 28 (2003) 1.
- 12 Kamkird P, Ketjoy N, Rakwichian W & Sukchai S, *Procedia Engineering*, 32 (2012) 376.
- 13 Kalogirou S A & Tripanagnostopoulos Y, *Energy Convers Manag*, 47 (2006) 3368.
- 14 Jordan D C, *Methods for analysis of outdoor performance data*, NREL PV Module Reliability Workshop, Colorado, USA, 16 February 2011.
- 15 Asian Power, Malaysia, September, 16 (2016). <http://asian-power.com/co-written-partner/more-news/find-out-what-igem-2016-will-reveal-solar-pv-industry>.

- 16 Atmospheric Science Data Center, *NASA Surface Meteorology and Solar Energy Location* (2017) <https://eosweb.larc.nasa.gov/cgi-bin/sse/grid.cgi>.
- 17 Breitenstein O, Bauer J, Trupke T & Bardos R A, *Prog Photovolt*, 16 (2008) 325.
- 18 Kajari-Schröder S, Kunze I, Eitner U & Köntges M, *Sol Energy Mater Sol Cells*, 95 (2011) 3054.
- 19 Takashi F, Hayato K, Tsutomu Y, Yu T & Yukiharu U, *Appl Phys Lett*, 86 (2005) 262108.
- 20 Würfel P, Trupke T, Puzzer T, Schäffer E, Warta W & Glunz S W, *J Appl Phys*, 101 (2007) 123110.
- 21 Mochizuki T, Kim C, Yoshita M, Mitchell J, Lin Z, Chen S, Takato H, Kanemitsu Y & Akiyama H, *J Appl Phys*, 119 (2016) 034501.
- 22 Sze M S & Ng K K, *Physics of semiconductor devices*, 3rd Edn, (John Wiley & Sons: India) 2007.
- 23 Bauer J, Frühauf F & Breitenstein O, *Sol Energy Mater Sol Cells*, 159 (2017) 8.
- 24 Dubey S & Tay A A O, *Energy Sustain Dev*, 17 (2013) 1.
- 25 Teo H G, Lee P S & Hawlader M N A, *Appl Energy*, 90 (2012) 309.
- 26 Rahman M M, Hasanuzzaman M & Rahim N A, *Energy Conv Manag*, 103 (2015) 348.
- 27 Mansouri A, Zettl M, Mayer O, Lynass M, Bucher M & Stern O, *Defect detection in photovoltaic modules using electroluminescence imaging*, 27th European Photovoltaic Solar Energy Conference and Exhibition, Frankfurt, Germany, 24 - 28 September 2012.
- 28 Frazão M, Silva J A, Lobato K & Serra J M, *Measurement*, 99 (2017) 7.
- 29 Chamberlin C E, Rocheleau M A, Marshall MW, Reis A M, Coleman N T, & Lehman P A, *Comparison of PV module performance before and after 11 and 20 years of field exposure*, 37th IEEE Photovoltaic Specialists Conference, Washington, USA, 19-24 June 2011.
- 30 Ndiaye A, Kébé C M F, Charki A, Ndiaye P A, Sambou V, & Kobi A, *Sol Energy*, 103 (2014) 70.
- 31 Limmanee A, Songtraai S, Udomdachanut N, Kaewnnyompanit S, Sato Y, Nakaishi M, Kittisontirak S, Sriprapha K & Sakamoto Y, *Renew Energy*, 102 (2017) 199.
- 32 Charrouf O, Betka A, Hadeif H, Djebabra M & Tiar M, *AIP Conf Proc*, 1814 (2017) 020030.
- 33 Hosenuzzaman M, *Energy, economic and environmental analyses of a solar energy based power generation under Malaysia conditions*, M Phil Thesis, University of Malaya, 2016.
- 34 International Energy Agency, *National Survey Report of PV Power Applications in Malaysia* (2015) http://www.iea-pvps.org/index.php?id=93&eID=dam_frontend_push&docID=2677.
- 35 Kumar B S & Sudhakar K, *Energy Reports*, 1 (2015) 184.
- 36 Sustainable Energy Development Authority (SEDA), Malaysia, *FiT rates for solar PV*, January (2017) <http://seda.gov.my>.
- 37 Rabii A B, Jraidi M & Bouazzi A S, *Investigation of the degradation in field-aged photovoltaic modules*, 3rd World Conference on Photovoltaic Energy Conversion, Osaka, Japan, 11-18 May 2003.
- 38 Singh P & Ravindra N M, *Sol Energy Mater Sol Cells*, 101 (2012) 36.